TOXICOLOGICAL SCIENCES **126(2)**, 487–496 (2012)
doi:10.1093/toxsci/kfr346
Advance Access publication January 4, 2012

# Differential Effects of 20 Non–Dioxin-Like PCBs on Basal and Depolarization-Evoked Intracellular Calcium Levels in PC12 Cells

Wendy T. Langeveld, Marieke Meijer, and Remco H.S. Westerink[1]

*Neurotoxicology Research Group, Institute for Risk Assessment Sciences, Utrecht University, NL-3508 TD Utrecht, The Netherlands*

[1]To whom correspondence should be addressed. Fax: +31-30-2535077. E-mail: r.westerink@uu.nl.

Received July 22, 2011; accepted December 19, 2011

**Non–dioxin-like polychlorinated biphenyls (NDL-PCBs) are environmental pollutants that are well known for their neurotoxic effects. Numerous *in vitro* studies reported PCB-induced increases in the basal intracellular calcium concentration ($[Ca^{2+}]_i$), and *in vivo* NDL-PCB neurotoxicity appears at least partly mediated by these disturbances. However, effects of NDL-PCBs on depolarization-evoked calcium influx are poorly investigated, and effects of several congeners, including PCB53, on calcium homeostasis are still unknown. We therefore studied the effects of 20 selected NDL-PCBs on basal and depolarization-evoked $[Ca^{2+}]_i$ in fura-2–loaded PC12 cells using single-cell fluorescence microscopy. The results demonstrate that hexa- and heptachlorobiphenyls (with the exception of PCB136) were unable to affect basal and depolarization-evoked $[Ca^{2+}]_i$. However, most tri- and tetrachlorinated as well as some pentachlorinated NDL-PCBs (at 1 and 10μM) increased basal $[Ca^{2+}]_i$ during a 15-min exposure. The increase in basal $[Ca^{2+}]_i$, which differed in kinetics for the different congeners, depended partly on influx of extracellular calcium and calcium release from the endoplasmic reticulum. Importantly, all tested tri- and tetrachlorinated biphenyls and some pentachlorinated NDL-PCBs (PCB95, PCB100, and PCB104) reduced depolarization-evoked $[Ca^{2+}]_i$, with PCB51 and PCB53 being most potent (near complete inhibition at 1μM). The reduction in depolarization-evoked calcium influx depended on the exposure duration but not on the foregoing PCB-induced increase in basal $[Ca^{2+}]_i$. The inhibition of voltage-gated calcium channels is a novel and sensitive mode of action for NDL-PCBs that contributes to the disturbances in calcium homeostasis and likely is related to NDL-PCB–induced (developmental) neurotoxicity.**

*Key Words:* **calcium homeostasis; depolarization-evoked calcium influx; voltage-gated calcium channel; single-cell fluorescence microscopy; NDL-PCB; PC12 cells.**

Polychlorinated biphenyls (PCBs) have been used in numerous industrial and commercial applications, but their use was largely prohibited in the 1970s and 1980s. Nonetheless, PCBs are still present in the environment and in biota, mainly because of improper disposal in combination with their lipophilicity and biopersistence (Agency for Toxic Substances and Disease Registry (ATSDR), 2000; Safe, 1993). PCBs are usually divided into coplanar dioxin-like (DL-) PCBs and non–dioxin-like (NDL-) PCBs. Contrary to DL-PCBs, NDL-PCBs have one or more chlorines in the *ortho*-positions, resulting in nonplanar structures. As a result, NDL-PCBs have little or no affinity to the aryl hydrocarbon receptor and display a different toxicological profile (ATSDR, 2000; Van den Berg *et al.*, 2006).

Epidemiological studies indicated that perinatal exposure to NDL-PCBs can result in neurodevelopmental and neurobehavioral effects in children (for review, see Faroon *et al.*, 2001; Schantz *et al.*, 2003; Winneke *et al.*, 2002). Moreover, *in vivo* studies have shown that animals dosed with NDL-PCBs displayed a range of neurobehavioral effects, including changes in motor activity, learning, memory, and attention (Boix *et al.*, 2010; Eriksson and Fredriksson, 1996; Holene *et al.*, 1998). *In vitro* studies identified several modes of action for NDL-PCBs, including inhibition of neurotransmitter uptake in synaptosomes and synaptic vesicles, alterations of neurotransmitter receptor expression as well as neurotransmitter levels the brain (for review, see Faroon *et al.*, 2001; Fonnum and Mariussen, 2009; Pessah *et al.*, 2010; Tilson and Kodavanti, 1998) and more recently modulation of neurotransmitter receptor function (Antunes Fernandes *et al.*, 2010; Hendriks *et al.*, 2010).

*In vitro* studies identified regulation of the intracellular calcium concentration ($[Ca^{2+}]_i$) as one of the critical parameters affected by NDL-PCBs (for review, see Fonnum and Mariussen, 2009; Pessah *et al.*, 2010; Tilson and Kodavanti, 1998). This is of significance for the neurotoxic potential of NDL-PCBs as $Ca^{2+}$ plays a crucial role in numerous cellular processes, including neurotransmission (for reviews, see Garcia *et al.*, 2006; Westerink, 2006), gene expression (for review, see Carrasco and Hidalgo, 2006), and cell death (for review, see Orrenius *et al.*, 2011). Consequently, neurons and neuroendocrine cells maintain low $[Ca^{2+}]_i$ at rest and exert strong control over the dynamics of their $Ca^{2+}$ signals, i.e., tightly regulate the balance between $Ca^{2+}$ influx, $Ca^{2+}$ extrusion, $Ca^{2+}$ sequestration, and $Ca^{2+}$ buffering by cytosolic $Ca^{2+}$-binding proteins (for reviews, see Berridge *et al.*, 2003; Garcia *et al.*, 2006; Westerink, 2006).

Until now, most studies focused on the effects of NDL-PCBs on maintenance of low basal $Ca^{2+}$ levels, and several NDL-PCBs have been shown to increase basal $[Ca^{2+}]_i$ (for review, see Fonnum and Mariussen, 2009; Pessah *et al*., 2010; Tilson and Kodavanti, 1998). Additional studies indicated that NDL-PCB–induced increases in $[Ca^{2+}]_i$ are most likely caused by release of $Ca^{2+}$ from the endoplasmic reticulum (ER) through activation of $IP_3$ and ryanodine (Ry) receptors (for review, see Pessah *et al*., 2010). Considering the abundance of studies on the effects of NDL-PCBs on basal $[Ca^{2+}]_i$, it is surprising that effects of NDL-PCBs on calcium dynamics during stimulation (depolarization) are hardly studied. Moreover, many congeners, including PCB51, PCB53, PCB74, PCB100, and PCB101, have not or only hardly been investigated for effects on $Ca^{2+}$ homeostasis. In the present study, we therefore investigated the effects of 21 PCBs on basal as well as depolarization-evoked $[Ca^{2+}]_i$ in rat PC12 cells. These cells are extensively characterized as an *in vitro* model to study changes in $Ca^{2+}$ homeostasis and presynaptic neurotransmission (for review, see Westerink and Ewing, 2008) and for *in vitro* neurotoxicity (for review, see Bal-Price *et al*., 2008). In undifferentiated PC12 cells, depolarization triggers a rapid increase in $[Ca^{2+}]_i$ that mainly originates from influx of $Ca^{2+}$ via high voltage–activated L-, N-, and P/Q-type $Ca^{2+}$ channels (Dingemans *et al*., 2009), and PC12 cells therefore provide an appropriate model for investigation of the effects of NDL-PCBs on $Ca^{2+}$ homeostasis. The selection of PCBs consists of 1 DL-PCB and 20 NDL-PCBs, selected based on their physical-chemical properties and abundance in food and human samples (Stenberg and Andersson, 2008).

## MATERIALS AND METHODS

***Chemicals.*** All chemicals were obtained from Sigma-Aldrich (St Louis, MO) unless otherwise noted. NaCl, KCl, and 4-(2-hydroxyethyl)-1-piperazineethanesulfonic acid (HEPES) were obtained from Merck (Whitehouse Station, NJ); $MgCl_2$, $CaCl_2$, glucose, sucrose, and NaOH were obtained from BDH Laboratory Supplies (Poole, U.K.); and Fura-2 AM was obtained from Molecular Probes (Invitrogen, Breda, The Netherlands). Highly purified (> 99.2%) PCBs were purchased from Neosync Inc., and possible impurities, e.g., polychlorinated dibenzodioxins/polychlorinated dibenzofurans (PCDD/Fs) and DL-PCBs, were removed by Stenberg and Andersson (Institute of Environmental Chemistry, Umeå University, Sweden) by applying a fractionation on active carbon cleanup step as described previously (Danielsson *et al*., 2008). The 21 PCBs used in this study were PCB19, PCB28, PCB47, PCB51, PCB52, PCB53, PCB74, PCB95, PCB100, PCB101, PCB104, PCB118, PCB122, PCB126, PCB128, PCB136, PCB138, PCB153, PCB170, PCB180, and PCB190 (see Table 1 for full names and number of *ortho*-chlorine substitutions of each congener). PCBs were dissolved in purity-checked dimethyl sulfoxide (DMSO) to obtain 25mM PCB stock solutions, which were further diluted immediately before experiments to obtain final concentrations of 1 and 10μM. The concentration of DMSO in PCB-containing saline was always kept below 0.1% (vol/vol) and DMSO at concentrations up to 0.5% (vol/vol) had no effect on intracellular calcium levels. Saline (containing in mM: 125 NaCl, 5.5 KCl, 2 $CaCl_2$, 0.8 $MgCl_2$, 10 HEPES, 24 glucose, and 36.5 sucrose at pH 7.3, adjusted with NaOH) was prepared with deionized water (Milli-Q; resistivity > 10 MΩ·cm).

***Cell culture.*** Undifferentiated rat pheochromocytoma (PC12) cells (Greene and Tischler, 1976; ATCC) were maintained in monolayers in 25 $cm^2$ tissue culture flasks (Nunc, Rochester, NY) in a humidified 5% $CO_2$/95% atmosphere air at 37°C in RPMI 1640 medium (Invitrogen) supplemented with 5% fetal calf serum, 10% horse serum (ICN Biomedicals, Zoetermeer, The Netherlands), 100 U/ml penicillin, and 100 μg/ml streptomycin (Invitrogen) as described previously (Dingemans *et al*., 2009; Hondebrink *et al*., 2011). Medium was refreshed every 2–3 days, and cells were cultured for up to 10 passages. Undifferentiated PC12 cells were subcultured in glass bottom dishes ($2 \times 10^5$ cells/dish; MatTek, Ashland, MA) for $[Ca^{2+}]_i$ imaging experiments as described previously (Dingemans *et al*., 2009; Hondebrink *et al*., 2011). All culture flasks and dishes were coated with poly-L-lysine (50 μg/ml).

***Fluorescent $Ca^{2+}$ imaging.*** Changes in $[Ca^{2+}]_i$ were measured using the $Ca^{2+}$-sensitive fluorescent ratio dye Fura-2 as described previously (Dingemans *et al*., 2009; Hondebrink *et al*., 2011). Briefly, cells were loaded with 8μM Fura-2 AM (Molecular Probes; Invitrogen) in saline for 20 min, followed by 20 min de-esterification in fresh saline. Cells were placed on the stage of an Axiovert 35M inverted microscope (Zeiss, Göttingen, Germany) equipped with a TILL Photonics Polychrome IV and an Image SensiCam digital camera (TILL Photonics GmBH, Gräfelfing, Germany). Camera and polychromator were controlled by imaging software (TILLvisION, version 4.01), which was also used for data collection and processing. All experiments were performed at room temperature (20°C–22°C).

Fluorescence was evoked by 340- and 380-nm excitation wavelengths (F340 and F380) and collected at 510 nm. The F340/F380 ratio ($R$), reflecting changes in $[Ca^{2+}]_i$, was measured every 3 s. At concentrations up to 10μM, PCBs do not affect the fluorescent characteristics of Fura-2 nor the overall absorbance (which could affect the excitation efficiency) of the PCB-containing saline at 340 and 380 nm.

Cells were continuously superfused with saline at a rate of ~0.6 ml/min using a ValveLink 8.2 perfusion system (AutoMate Scientific, Berkeley, CA). Each experiment consisted of a 5-min baseline recording to measure basal $[Ca^{2+}]_i$, after which an increase in $[Ca^{2+}]_i$ was triggered by changing superfusion to 100mM $K^+$ for 20 s. Following this first depolarization and an 8-min recovery period, cells were exposed to DMSO-containing saline (control) or PCB-containing saline (1 or 10μM) for 15 min prior to a second depolarization with 100mM $K^+$- (control) or 100mM $K^+$- and PCB-containing saline (see Figs. 1 and 2 for example recordings).

For specific experiments, cells were maintained in $Ca^{2+}$-free saline to determine the involvement of $Ca^{2+}$ influx in the observed PCB-induced effects on basal $[Ca^{2+}]_i$. In further experiments, cells were incubated with thapsigargin (TG, 1μM) under $Ca^{2+}$-free conditions to deplete ER prior to PCB exposure to identify the involvement of intracellular $Ca^{2+}$ stores. Separate experiments were performed to identify direct effects of PCBs on voltage-gated calcium channels (VGCCs). In these experiments, PCBs were present only during the second depolarization.

***Data analysis and statistics.*** Data were analyzed using custom-made MS-Excel macros. Free cytosolic $[Ca^{2+}]_i$ was calculated according to a modified Gronkiewicz's equation $[Ca^{2+}]_i = K_{d*} \times (R - R_{min})/(R_{max} - R)$ where maximum and minimum ratios ($R_{max}$ and $R_{min}$) were determined after the recording by addition of ionomycin (5μM) and EDTA (17mM) and $K_{d*}$ is the dissociation constant of Fura-2 determined in the experimental setup (Deitmer and Schild, 2000). Cells that showed $[Ca^{2+}]_i$ 2× SD above or below average, either during basal recording or during depolarization, were excluded from further analysis (~17%).

The PCB exposure was divided in an early (0–3 min), mid (4–7 min), and late (8–15 min) phase of exposure to temporally characterize the change in basal $[Ca^{2+}]_i$. The amplitude of the second $K^+$-evoked increase in $[Ca^{2+}]_i$ (after 15 min of PCB exposure) was expressed as a percentage of the amplitude of the first $K^+$-evoked increase in $[Ca^{2+}]_i$ per cell to obtain a "treatment ratio" (TR) as described previously (Hondebrink *et al*., 2011; for illustration, see Fig. 1). As persistent changes in basal $[Ca^{2+}]_i$ can influence

the amplitude of the second $K^+$-evoked increase in $[Ca^{2+}]_i$, a net $K^+$-evoked increase in $[Ca^{2+}]_i$ was calculated by subtracting the amplitude of $[Ca^{2+}]_i$ just prior to depolarization from the amplitude of the $K^+$-evoked increase in $[Ca^{2+}]_i$. Net increases in $K^+$-evoked increases in $[Ca^{2+}]_i$ were used to derive a "net TR."

As the SD for basal $[Ca^{2+}]_i$ and TR amounted to 17 and 21%, respectively, effects < 25% were considered irrelevant; all relevant effects are statistically significant ($p < 0.05$; Student's *t*-test, paired or unpaired where applicable). Unless otherwise indicated, data are presented as mean ± SD of *n* cells obtained from *N* independent experiments.

## RESULTS

### *Effects of NDL-PCBs on Basal $[Ca^{2+}]_i$*

Basal $[Ca^{2+}]_i$ of control cells superfused with saline for 5 min was stable and amounted to 99 ± 17nM ($n = 317$; $N = 47$; see also Fig. 1). $[Ca^{2+}]_i$ increased rapidly and transiently to 1.80 ± 0.64μM upon 20 s superfusion with 100mM $K^+$-containing saline to depolarize the cells. During a subsequent 8-min recovery period, $[Ca^{2+}]_i$ returned to near resting values. Prior to a second depolarization, cells were exposed to DMSO-containing saline for 15 min, which did not affect $[Ca^{2+}]_i$ (Fig. 1).

When cells were exposed to PCB-containing saline for 15 min prior to the second depolarization with 100mM $K^+$, several different effects on $[Ca^{2+}]_i$ could be observed, including fast transient as well as slowly developing increases in $[Ca^{2+}]_i$ (Figs. 2 and 3; Table 1). A number of NDL-PCBs did not induce clear effects on basal $[Ca^{2+}]_i$ either at 1μM or at 10μM (Fig. 3). This group of PCBs consisted mainly of higher chlorinated NDL-PCBs, including all tested hexa- and heptachlorobiphenyls (with the exception of PCB136) as well as some pentachlorinated (PCB104, PCB118, PCB122, and the DL-PCB126) and one tetrachlorinated biphenyl (PCB74). At 10μM, the other tested tri- and tetrachlorobiphenyls increased basal $[Ca^{2+}]_i$. These effects were generally less pronounced or absent at 1μM, though for PCB52, PCB53, and PCB95, basal $[Ca^{2+}]_i$ is already strongly increased at 1μM. At 10μM, exposure to PCB19 and PCB53 clearly resulted in an early increase in basal $[Ca^{2+}]_i$ that diminished over time (Figs. 2 and 3). On the other hand, exposure to PCB47, PCB51, PCB52, PCB95, and PCB136 increased basal $[Ca^{2+}]_i$ mainly in the mid and late phase of exposure (Figs. 2 and 3). PCB28 was difficult to classify because the increase in $[Ca^{2+}]_i$ was limited, but it seemed that PCB28 also falls into the "late" category, along with PCB100 and PCB101, which only showed modest increases in $[Ca^{2+}]_i$ in the late phase of exposure (Fig. 3).

A subset of NDL-PCBs (PCB19, PCB53, and PCB95) that induced pronounced effects on basal $[Ca^{2+}]_i$ was used to confirm in additional experiments that the mechanisms underlying the observed increase in basal $[Ca^{2+}]_i$ involved intracellular $Ca^{2+}$ stores as demonstrated previously (for review, see Fonnum and Mariussen, 2009; Pessah *et al.*, 2010; Tilson and Kodavanti, 1998). Indeed, when cells were exposed to the selected NDL-PCBs in $Ca^{2+}$-free medium, the increase in basal $[Ca^{2+}]_i$ was reduced but still present (not shown), thereby indicating that the increase in $[Ca^{2+}]_i$ originated from intracellular stores. To further investigate the involvement of intracellular $Ca^{2+}$-stores, cells were pretreated with thapsigargin (TG) in $Ca^{2+}$-free medium to empty the ER prior to PCB exposure. Upon exposure to TG (1μM), a transient increase in $[Ca^{2+}]_i$ was observed, representing $Ca^{2+}$ release from the ER. When these pretreated cells were subsequently exposed to the selected NDL-PCBs, $[Ca^{2+}]_i$ no longer increased (not shown),

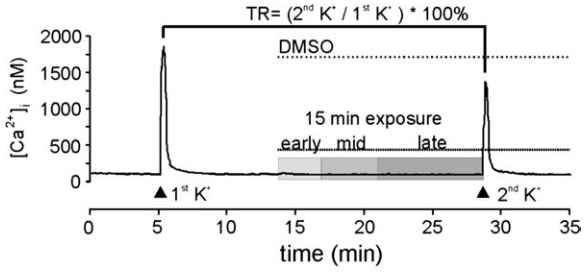


**FIG. 1.** Representative example recordings of $[Ca^{2+}]_i$ from an individual PC12 cell exposed for 15 min to DMSO-containing saline as indicated by the dotted line in the recording. The cell is depolarized with 100mM $K^+$-containing saline (indicated by the arrowheads below the traces) before and at the end of the exposure period. This allows for calculation of a TR (see Materials and Methods section for details) to investigate the effects of exposure to the different congeners on depolarization-evoked $Ca^{2+}$ influx.

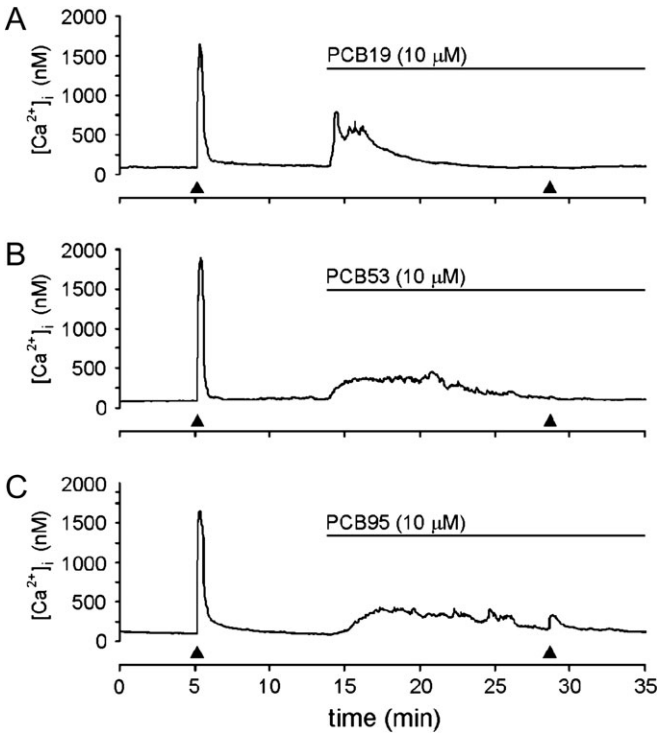


**FIG. 2.** PCB-induced effects on basal and depolarization-evoked $[Ca^{2+}]_i$. Representative example recordings of $[Ca^{2+}]_i$ from individual PC12 cells exposed for 15 min to saline containing PCB19 (A), PCB53 (B), or PCB95 (C) at 10μM as indicated by the solid line on top of the recordings. Cells are depolarized with 100mM $K^+$-containing saline (indicated by the arrowheads below the traces) before and at the end of the exposure period to investigate the effects of the different congeners on depolarization-evoked $Ca^{2+}$ influx.

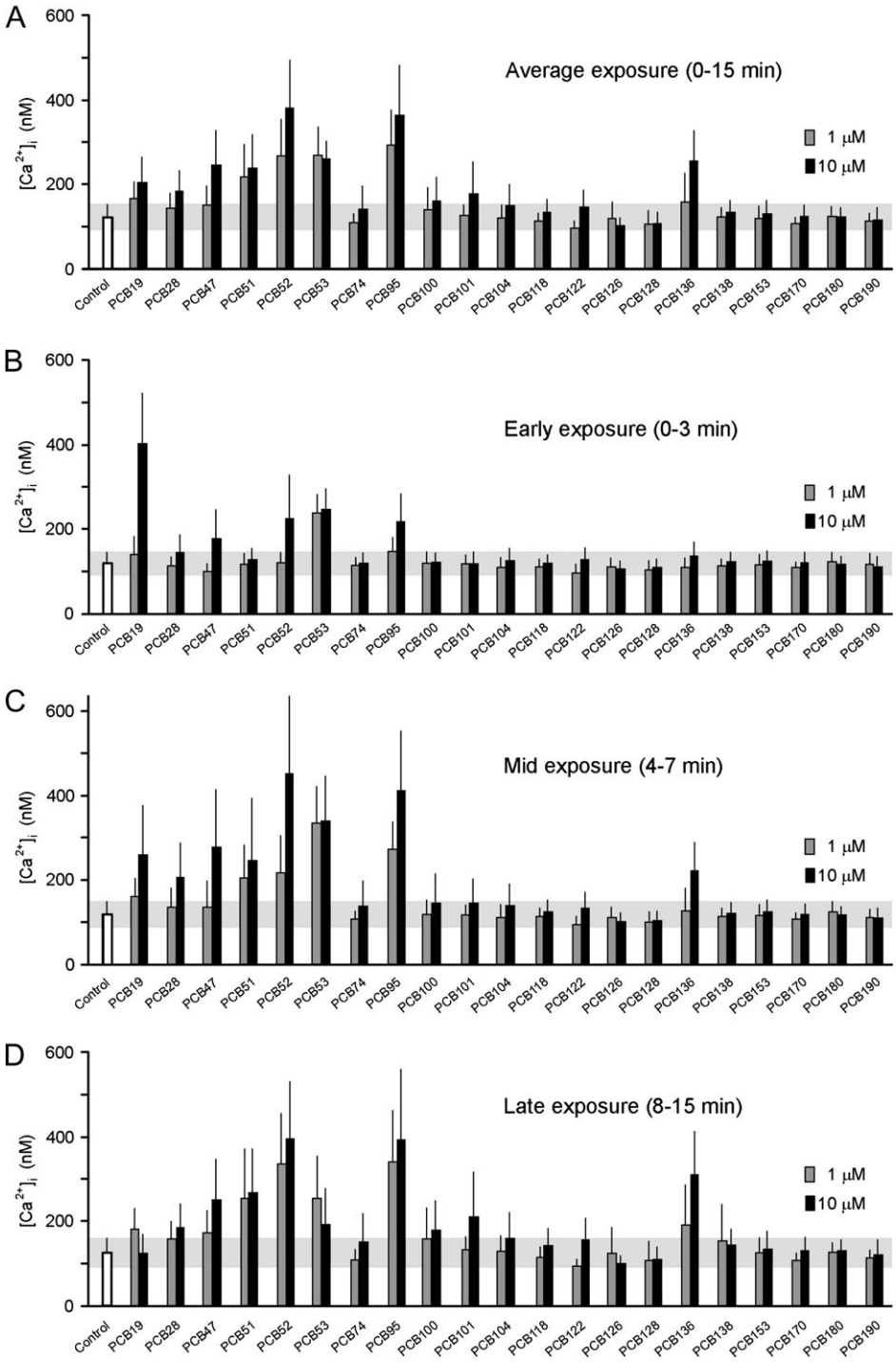


**FIG. 3.** Summary graphs of PCB-induced effects on basal $[Ca^{2+}]_i$ in PC12 cells. (A) Average amplitude of $[Ca^{2+}]_i$ during 15 min exposure (in between the 2 depolarizations) to DMSO (control) or one of the 21 congeners at 1 or 10μM. (B) Average amplitude of $[Ca^{2+}]_i$ in the early phase of exposure (0–3 min). PCB19 and PCB53 already show a clear increase in basal $[Ca^{2+}]_i$. (C) Average amplitude of $[Ca^{2+}]_i$ in the mid phase of exposure (4–7 min). The PCB19-induced increase in basal $[Ca^{2+}]_i$ is already diminishing, whereas the PCB53-induced basal $[Ca^{2+}]_i$ is even more profound. Also PCB52, PCB95, and to a lesser extent PCB28, PCB47, PCB51, and PCB136 increase basal $[Ca^{2+}]_i$ in this phase. (D) Average amplitude of $[Ca^{2+}]_i$ in the late phase of exposure (8–15 min). In particular, PCB52, PCB95, and PCB136 show a profound increase in basal $[Ca^{2+}]_i$ in this phase. Effects smaller than control ± SD (indicated by the shaded area) are considered irrelevant. Bars indicate mean ± SD of 317 control cells ($N = 47$) or of 25–50 congener-exposed cells ($N = 3$–8).

confirming that the increase in basal $[Ca^{2+}]_i$ originated from the ER (for review, see Fonnum and Mariussen, 2009; Pessah *et al.*, 2010; Tilson and Kodavanti, 1998).

### *Effects of NDL-PCBs on Depolarization-Evoked Increases in $[Ca^{2+}]$*

Following 15-min exposure to DMSO-containing saline, control cells showed a fast transient increase in $[Ca^{2+}]_i$ upon a second depolarization with 100mM $K^+$ for 20 s that amounted to ~75% (1.39 ± 0.62μM) of the first depolarization (Fig. 1). As the amplitude of the depolarization-evoked $[Ca^{2+}]_i$ could be influenced by a prolonged PCB-induced increase in basal $[Ca^{2+}]_i$, a net TR was calculated. For control cells, net TR amounted to 73 ± 21% ($n = 317$; $N = 47$).

A number of NDL-PCBs did not affect depolarization-evoked $Ca^{2+}$ influx, neither at 1μM nor at 10μM (Fig. 4; Table 1). This group of PCBs consisted mainly of higher chlorinated NDL-PCBs, including all tested hexa- and heptachlorobiphenyls (with the exception of PCB136) but also some pentachlorobiphenyls (PCB101, PCB118, PCB122, and the DL-PCB126). At 10μM, all tested tri- and tetrachlorobiphenyls as well as some pentachlorobiphenyls (PCB95, PCB100, and PCB104) inhibited depolarization-evoked $Ca^{2+}$ influx. At 1μM, the inhibition of depolarization-evoked $Ca^{2+}$ influx was generally smaller, though some PCBs (PCB47, PCB51, PCB53, and PCB104) already strongly inhibited $Ca^{2+}$ influx at this lower concentration. This holds in particular for PCB51, which at 1μM already reduced net TR by ~90% (Fig. 4).

At 10μM, PCB19 and PCB53 induced a large transient increase in basal $[Ca^{2+}]_i$ as well as a strong reduction in depolarization-evoked $Ca^{2+}$ influx (Figs. 2–4). The inhibition of depolarization-evoked $Ca^{2+}$ influx could thus be (partly) due to the foregoing PCB-induced increase in basal $[Ca^{2+}]_i$. However, when cells were exposed to 10μM PCB19 or PCB53 only during the second depolarization, the net TR was indistinguishable from control cells (not shown). This indicated that the reduction in depolarization-evoked $Ca^{2+}$ influx depended on the duration of the PCB exposure and/or PCB-induced increase in basal $[Ca^{2+}]_i$. The latter is unlikely as some NDL-PCBs (PCB74 and PCB104 [10μM]) inhibited depolarization-evoked $Ca^{2+}$ influx in the absence of effects on basal $[Ca^{2+}]_i$ (Figs. 3 and 4). However, when cells were exposed to 10μM PCB74 or PCB104 only during the second depolarization, the net TR was also not different from control (not shown), indicating that the reduction in depolarization-evoked $Ca^{2+}$ influx depended on exposure duration rather than on a foregoing increase in basal $[Ca^{2+}]_i$.

### *Effects of Low-Dose and Binary Mixtures of PCB53 and PCB95 on Basal and Depolarization-Evoked Increases in $[Ca^{2+}]_i$*

This study was designed to investigate effects of different NDL-PCBs on basal and depolarization-evoked $[Ca^{2+}]_i$ and possible structure-activity relationships. However, some of the selected NDL-PCBs appear very potent in disturbing $[Ca^{2+}]_i$. We therefore selected PCB53 and PCB95 for additional experiments at lower concentrations, as these PCBs show potent effects at both basal and depolarization-evoked $[Ca^{2+}]_i$. Figure 5A illustrates the effects of PCB53 and PCB95 at 0.1, 1, and 10μM. Also at 0.1μM, both PCBs already show a clear increase in the basal $[Ca^{2+}]_i$. On the other hand, the inhibition of depolarization-evoked $[Ca^{2+}]_i$ is absent at this concentration (Fig. 5B), and for PCB53, even a modest potentiation of the depolarization-evoked $[Ca^{2+}]_i$ can be observed.

Next, we tested the effects of a binary mixture of PCB53 and PCB95 (both at 0.1μM) on basal and depolarization-evoked $[Ca^{2+}]_i$ (Fig. 6). It is clear from Figure 6A that the effects of both PCBs on basal $[Ca^{2+}]_i$ apparently are not additive. On the other hand, the slight potentiation of depolarization-evoked $[Ca^{2+}]_i$ by 0.1μM PCB53 (120 ± 57% [$n = 36$; $N = 4$]) and 0.1μM PCB95

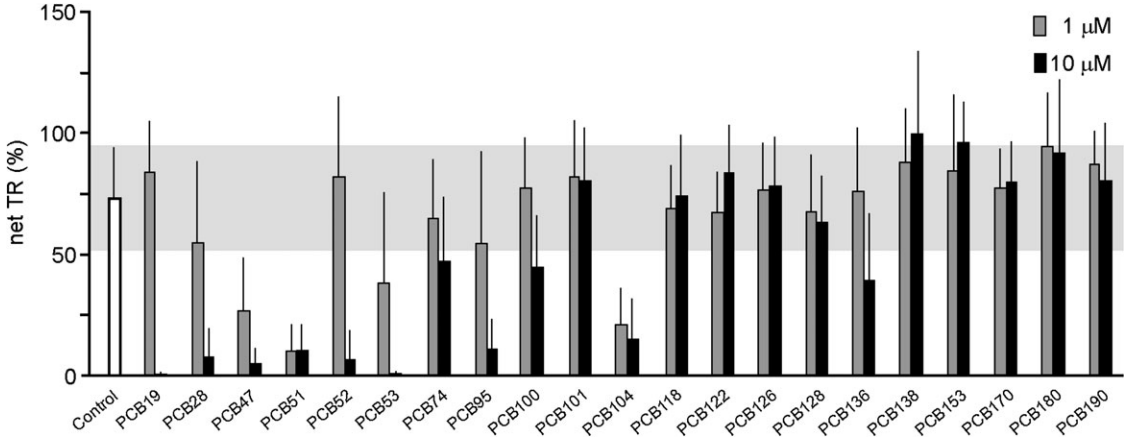


**FIG. 4.** Summary graph of PCB-induced effects on depolarization-evoked $[Ca^{2+}]_i$ in PC12 cells. The net TR (see Materials and Methods for details) is used as a measure for inhibition of depolarization-evoked $Ca^{2+}$ influx. The reduction in net TR is particular profound for the tested tri- and tetrachlorinated biphenyls. Effects smaller than control ± SD (indicated by the shaded area) are considered irrelevant. Bars indicate mean ± SD of 317 control cells ($N = 47$) or of 25–50 congener-exposed cells ($N = 3$–8).

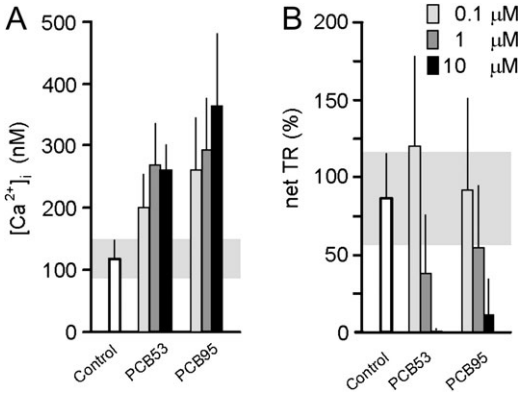


**FIG. 5.** Summary graph illustrating the dose dependence (0.1–10μM) of effects of PCB53 and PCB95 on basal (A) and depolarization-evoked $[Ca^{2+}]_i$ (B) in PC12 cells. Effects smaller than control ± SD (indicated by the shaded area) are considered irrelevant. Bars indicate mean ± SD of 88 control cells ($N = 10$) or of 25–46 congener-exposed cells ($N = 4$–5).

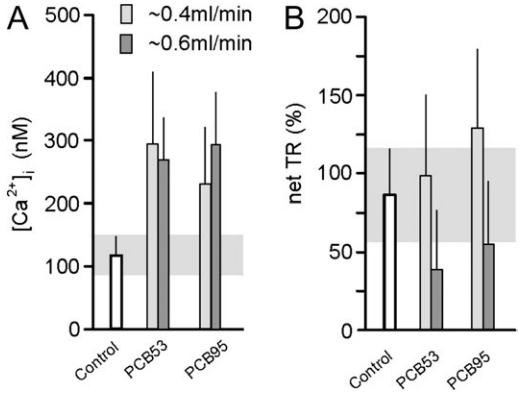


**FIG. 7.** Summary graph illustrating the effects of the rate of superfusion with PCB53 (1μM) and PCB95 (1μM) on basal (A) and depolarization-evoked $[Ca^{2+}]_i$ (B) in PC12 cells. Effects smaller than control ± SD (indicated by the shaded area) are considered irrelevant. Bars indicate mean ± SD of 88 control cells ($N = 10$) or of 25–26 congener-exposed cells ($N = 4$).

(94 ± 65% [$n = 46$; $N = 5$]) appears to be additive (Fig. 6B), amounting to 142 ± 42% ($n = 34$; $N = 4$) for the binary mixture compared with 85 ± 32% ($n = 88$; $N = 10$) for control cells (Fig. 6B).

Interestingly, the rate of superfusion appeared to be of considerable importance for the degree of PCB-induced effects. When we reduced the rate of superfusion from ~0.6 to ~0.4 ml/min, basal and depolarization-evoked $[Ca^{2+}]_i$ were unaffected in DMSO-exposed control cells (not shown). Similarly, this reduction in flow speed was rather ineffective in altering the effects of PCB53 and PCB95 on basal $[Ca^{2+}]_i$ (Fig. 7A). However, the effects of PCB53 and PCB95 on depolarization-evoked $[Ca^{2+}]_i$ became less pronounced at a lower rate of superfusion (Fig. 7B), clearly stressing the need for carefully controlled PCB exposure.

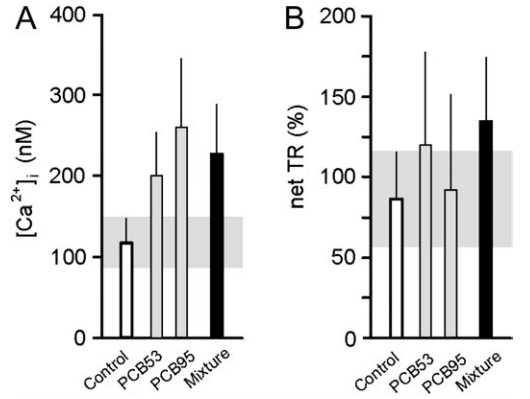


**FIG. 6.** Summary graph illustrating the effects of a binary mixture of PCB53 (0.1μM) and PCB95 (0.1μM) on basal (A) and depolarization-evoked $[Ca^{2+}]_i$ (B) in PC12 cells. Effects smaller than control ± SD (indicated by the shaded area) are considered irrelevant. Bars indicate mean ± SD of 88 control cells ($N = 10$) or of 25–46 congener-exposed cells ($N = 4$–5).

## DISCUSSION

NDL-PCBs are well known for their neurotoxic potential, in particular disturbance of neuronal calcium homeostasis (for review, see Fonnum and Mariussen, 2009; Pessah *et al.*, 2010; Tilson and Kodavanti, 1998). Previously, it has been shown that basal $[Ca^{2+}]_i$ is increased upon acute exposure to several NDL-PCBs or commercially available PCB mixtures, such as low micromolar concentrations of Aroclor 1254 (Inglefield *et al.*, 2001). Of the investigated NDL-PCBs, PCB95 is among the most well-studied and potent PCBs with respect to disturbing basal $[Ca^{2+}]_i$ (Wong and Pessah, 1997; Wong *et al.*, 2001). Most *in vitro* studies suggest a clear involvement of the ER in the observed increase in $[Ca^{2+}]_i$, mainly through activation of $IP_3$ and Ry receptors (for review, see Fonnum and Mariussen, 2009; Pessah *et al.*, 2010).

Our study, using a selection of 20 highly purified NDL-PCBs, confirms and extends on these results. The tested hexa- and heptachlorobiphenyls (at 1 or 10μM) did not affect basal $[Ca^{2+}]_i$ during 15 min exposure (Fig. 3). PCB136 appears to be an exception as it was the only hexachlorobiphenyl that induced an increase in $[Ca^{2+}]_i$ at least in the mid and late phase of exposure (4–15 min). Most pentachlorinated NDL-PCBs also showed no or very limited effects on basal $[Ca^{2+}]_i$ with the exception of PCB95, which has previously been shown to increase basal $[Ca^{2+}]_i$ (Wong and Pessah, 1997; Wong *et al.*, 2001). PCB95 effectively increased $[Ca^{2+}]_i$ during the mid and late phase of exposure (4–15 min) already at 1μM (Figs. 2 and 3). Except PCB74, all tested tri- and tetrachlorobiphenyls increased basal $[Ca^{2+}]_i$ to some extent. PCB19 and PCB53 proved very efficient in increasing basal $[Ca^{2+}]_i$ in the early phase of exposure (0–3 min). The effects of PCB19 were transient and virtually absent in the mid and late phase of exposure, whereas the effects of PCB53 were more persistent. On the other hand, PCB51 and PCB52 showed hardly any effect during the early phase of exposure but increased basal $[Ca^{2+}]_i$ mainly during

**TABLE 1**

**Overview of Full Names, Number of *ortho*-substitutions, Structure, and Effects on Basal and Depolarization-Evoked $[Ca^{2+}]_i$ of the Congeners Used in the Present Study**

| Congener (number of *ortho*-substitutions), full name | Structure | Increase in basal $[Ca^{2+}]_i$ | | Inhibition VGCCs | |
|---|---|---|---|---|---|
| | | 1μM | 10μM | 1μM | 10μM |
| PCB19 (tri-*ortho*), 2,2′,6-Trichlorobiphenyl | 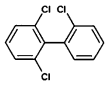 | + | +++ | NE | +++ |
| PCB28 (mono-*ortho*), 2,4,4′-Trichlorobiphenyl | 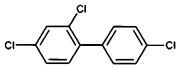 | NE | + | NE | +++ |
| PCB47 (di-*ortho*), 2,2′,4,4′-Tetrachlorobiphenyl | 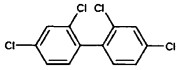 | + | ++ | ++ | +++ |
| PCB51 (tri-*ortho*), 2,2′,4,6′-Tetrachlorobiphenyl | 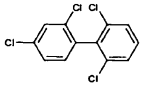 | ++ | ++ | +++ | +++ |
| PCB52 (di-*ortho*), 2,2′,5,5′-Tetrachlorobiphenyl | 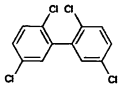 | ++ | +++ | NE | +++ |
| PCB53 (tri-*ortho*), 2,2′,5,6′-Tetrachlorobiphenyl | 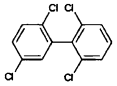 | +++ | +++ | ++ | +++ |
| PCB74 (mono-*ortho*), 2,4,4′,5-Tetrachlorobiphenyl | 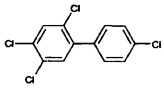 | NE | NE | NE | + |
| PCB95 (tri-*ortho*), 2,2′,3,5′,6-Pentachlorobiphenyl | 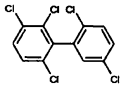 | +++ | +++ | + | ++ |
| PCB100 (tri-*ortho*), 2,2′,4,4′,6-Pentachlorobiphenyl | 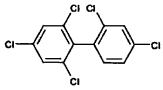 | NE | + | NE | + |
| PCB101 (di-*ortho*), 2,2′,4,5,5′-Pentachlorobiphenyl | 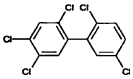 | NE | + | NE | NE |
| PCB104 (tetra-*ortho*), 2,2′,4,6,6′-Pentachlorobiphenyl | 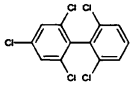 | NE | NE | ++ | ++ |
| PCB118 (mono-*ortho*), 2,3′,4,4′,5-Pentachlorobiphenyl | 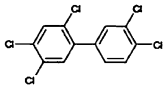 | NE | NE | NE | NE |
| PCB122 (mono-*ortho*), 2′,3,3′,4,5,-Pentachlorobiphenyl | 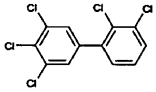 | NE | NE | NE | NE |
| PCB128 (di-*ortho*), 2,2′,3,3′,4,4′-Hexachlorobiphenyl | 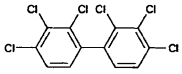 | NE | NE | NE | NE |
| PCB136 (tetra-*ortho*), 2,2′,3,3′,6,6′-Hexachlorobiphenyl | 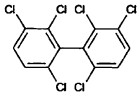 | + | ++ | NE | + |
| PCB138 (di-*ortho*), 2,2′,3,4,4′,5′-Hexachlorobiphenyl | 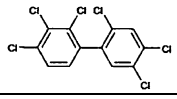 | NE | NE | NE | NE |

**TABLE 1—*Continued***

| Congener (number of *ortho*-substitutions), full name | Structure | Increase in basal $[Ca^{2+}]_i$ | | Inhibition VGCCs | |
|---|---|---|---|---|---|
| | | 1μM | 10μM | 1μM | 10μM |
| PCB153 (di-*ortho*), 2,2′,4,4′,5,5′-Hexachlorobiphenyl | 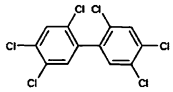 | NE | NE | NE | NE |
| PCB170 (di-*ortho*), 2,2′,3,3′,4,4′,5-Heptachlorobiphenyl | 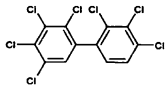 | NE | NE | NE | NE |
| PCB180 (di-*ortho*), 2,2′,3,4,4′,5,5′-Heptachlorobiphenyl | 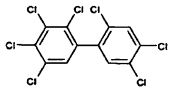 | NE | NE | NE | NE |
| PCB190 (di-*ortho*), 2,3,3′,4,4′,5,6,-Heptachlorobiphenyl | 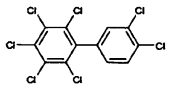 | NE | NE | NE | NE |
| PCB126 (non-*ortho*), 3,3′,4,4′,5-Pentachlorobiphenyl | 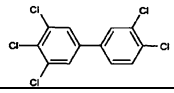 | NE | NE | NE | NE |

*Note*. +, mild effect; ++, moderate effect; +++, strong effect; NE, no effect. Criteria for selection of the different congeners are described in Stenberg and Andersson (2008).

the late phase (8–15 min). The different NDL-PCBs thus affect basal $[Ca^{2+}]_i$ with different kinetics, which together with differences in purity and recording techniques could explain some of the controversies existing in literature. Additional discrepancies in literature may be due to differences in exposure scenario, as the rate of superfusion is clearly of potential influence on the results (Fig. 7). Though NDL-PCBs increase basal $[Ca^{2+}]_i$ with different kinetics, they apparently share the underlying mechanism, which involves influx of extracellular calcium and release of calcium from ER as the effects PCB19 (trichlorobiphenyl), PCB53 (tetrachlorobiphenyl), and PCB95 (pentachlorobiphenyl) were reduced in $Ca^{2+}$-free medium and abolished following depletion of the ER as demonstrated previously for several other NDL-PCBs (for review, see Fonnum and Mariussen, 2009; Pessah *et al.*, 2010).

Our study thus demonstrates that tri- and tetrachlorobiphenyls, including the not previously tested PCB53, can efficiently increase basal $[Ca^{2+}]_i$. Importantly, our experimental design not only allows for a temporal characterization of the increase in basal $[Ca^{2+}]_i$ on a single-cell basis but also allows for investigation of possible effects of NDL-PCBs on a subsequent depolarization. Our data (Figs. 2 and 4) demonstrate inhibition of depolarization-evoked calcium influx as a novel mode of action of some NDL-PCBs. Moreover, some NDL-PCBs inhibited calcium influx very effectively already at 1μM (e.g., PCB51). The inhibition of calcium influx apparently depended on exposure duration, but not on the presence of a foregoing increase in basal $[Ca^{2+}]_i$ as some NDL-PCBs have no effect on ER calcium stores, i.e., do not increase basal calcium levels, yet clearly inhibit depolarization-evoked calcium entry (e.g., PCB104 at 1 and 10μM, PCB74 at 10μM, and PCB47 at 1μM; also see Results section). This indicates that PCBs inhibit VGCCs possibly via accumulation in the cell membrane and subsequent alteration of membrane characteristics (e.g., fluidity) resulting in a nonspecific inhibition of VGCCs. Alternatively, PCBs have to enter the cell first (transmembrane or channel mediated) to subsequently inhibit VGCCs by binding to a cytosolic domain of the VGCCs. Because the inhibition of $Ca^{2+}$ influx amounted up to ~99% for some congeners, the block of VGCCs is not specific for a subtype of VGCCs, e.g., L- or N-type VGCCs. It is therefore less likely that PCB-induced inhibition of VGCCs involved a second messenger pathway as this would usually not result in a complete inhibition of all VGCCs subtypes (for review, see Westerink, 2006).

Though the current study was not designed to derive complete dose-response curves for the effects of the 20 selected NDL-PCBs on basal and depolarization-evoked $[Ca^{2+}]_i$, it is possible to derive a limited rank-order potency (see also Table 1). PCB53 (tri-*ortho*-substituted tetrachlorobiphenyl), PCB95 (tri-*ortho*-substituted pentachlorobiphenyl), and to a lesser extent PCB52 (di-*ortho*-substituted tetrachlorobiphenyl) induced a robust increase in basal $[Ca^{2+}]_i$ already at 1μM, albeit with different kinetics. With the exception of PCB95 and PCB136, activity appears generally limited to di- and tri-*ortho*-substituted trichlorobiphenyls and tetrachlorobiphenyls. In line with previously established structure-activity relationships established for activation of Ry type 1 receptors (Pessah *et al.*, 2006), *para*-substitutions appear to lower the activity. Except PCB136, hexa- and heptachlorobiphenyls were ineffective in increasing basal $[Ca^{2+}]_i$ (Fig. 2; Table 1), though, e.g., PCB170 and PCB180

showed considerable activity on Ry type 1 receptors (Pessah *et al.*, 2006). These differences are likely due to differences in models system and especially in exposure duration (15-min exposure in intact cells to determine effects on basal $[Ca^{2+}]_i$ in our study vs. up to 3 h exposure in microsomes to determine Ry receptor activity). It is thus not unlikely that some of the higher chlorinated NDL-PCBs increase $[Ca^{2+}]_i$ following a more prolonged exposure, especially since the lipophilicity and thus bioavailability of NDL-PCBs generally increases with increasing chlorination number (see, e.g., Khadikar *et al.*, 2002). Nonetheless, our data clearly show that tri-, tetra-, and some pentachlorinated congeners are most potent (Figs. 3 and 4), and it is therefore not likely that the observed effects are simply due to differential bioavailability.

PCB51, together with PCB47, PCB53, and PCB104, is most potent in inhibiting VGCCs. These congeners produce a strong inhibition already at 1μM. Comparable with the effects on basal $[Ca^{2+}]_i$, inhibition of VGCCs appears mainly limited to di- and tri-*ortho*-substituted trichlorobiphenyls and tetrachlorobiphenyls, with the exception of PCB104 which is ineffective in increasing basal $[Ca^{2+}]_i$ but is fairly potent in inhibiting VGCCs. As the inhibition of VGCCs clearly depends on the exposure duration, prolonged exposure may identify additional (higher chlorinated) NDL-PCBs that are capable of inhibiting VGCCs.

The PCB-induced increases in basal $[Ca^{2+}]_i$ likely play a role in previously observed effects on gene expression and cell death (for review, see Fonnum and Mariussen, 2009) as numerous neuronal processes, including long-term potentiation, synaptic plasticity, neurotransmission, neurodegeneration, and neurodevelopment, critically depend on proper calcium homeostasis (for reviews, see Catterall and Few, 2008; Malenka and Nicoll, 1999; Mattson, 2007; Michaelsen and Lohmann, 2010; Westerink, 2006). It is therefore not unlikely that the PCB-induced inhibition of VGCCs plays a significant role in the neurodevelopmental and neurobehavioral impairments observed following *in vivo* PCB exposure (for review, see Faroon *et al.*, 2001; Schantz *et al.*, 2003; Winneke *et al.*, 2002).

Humans are exposed to PCBs mainly via the diet (European Food Safety Authority, 2005), although inhalation of (indoor) air and house dust can be a significant route of exposure, especially for lower chlorinated congeners (Broding *et al.*, 2007; Harrad *et al.*, 2010). Resulting levels of individual PCBs in human blood are generally in the low nanomolar range (Gabrio *et al.*, 2000; Petrik *et al.*, 2006). The concentrations used in the present study are thus ~2 to 3 orders of magnitude higher than those found in humans. Though lowest observed effect concentrations (LOECs) were not derived in this study, it is clear that some congeners, including PCB47, PCB51, PCB52, PCB53, PCB95, and PCB104, induce robust increases in basal $[Ca^{2+}]_i$ and inhibition of VGCCs already at 1μM. PCB53 and PCB95 increase basal $[Ca^{2+}]_i$ also at 0.1μM (Fig. 5). The LOECs for the more potent PCBs (PCB47, PCB51, PCB52, PCB53, PCB95, PCB104, and to a lesser extent PCB136) are thus expected to be in the nanomolar range. Moreover, considering the clear dependence on exposure duration as well as the bioaccumulative properties of PCBs, it is possible that a longer exposure scenario results in reduced LOECs. Finally, it is not unlikely that additivity occurs, further lowering the margin of safety. However, our initial data on the increase in basal $[Ca^{2+}]_i$ induced by a mixture of PCB53 and PCB95 indicates that at least for these two NDL-PCBs additivity may not apply (Fig. 6).

Additional research is required to establish the LOECs for the observed effects, especially following prolonged exposure, and to determine whether or not additivity applies, especially at low concentrations. Our data (Table 1) can be used to identify a test set of potent congeners that would be suited for this purpose (PCB19, PCB47, PCB51, PCB52, PCB53, PCB95, PCB104, and PCB136). Moreover, the current data unequivocally extend on the known effects of NDL-PCBs on calcium homeostasis and identify inhibition of VGCCs as a novel and sensitive mode of action for di- and tri-*ortho*-substituted lower chlorinated NDL-PCBs. Though environmental and human serum levels of PCBs may be declining, the current findings are likely to be of particular relevance for developing children as the developing nervous system is more vulnerable and young children have a relatively high exposure.

## FUNDING

This research was funded by the European Union (Assessing the Toxicity and Hazard Of Non-dioxin-like PCBs present in food [ATHON], Grant Agreement FOOD-CT-2005-022923) and the faculty of veterinary sciences of Utrecht University.

## ACKNOWLEDGMENTS

We thank Dr E. C. Antunes Fernandes and the members of the neurotoxicology research group for helpful discussions.

## REFERENCES

Agency for Toxic Substances and Disease Registry (ATSDR). (2000). Toxicological Profile for Polychlorinated Biphenyls (PCBs). Agency for Toxic Substances & Disease Registry, Atlanta, GA.

Antunes Fernandes, E. C., Hendriks, H. S., van Kleef, R. G. D. M., Reniers, A., Andersson, P. L., van den Berg, M., and Westerink, R. H. S. (2010). Activation and potentiation of human $GABA_A$ receptors by non-dioxin-like PCBs depends on chlorination pattern. *Toxicol. Sci.* **118,** 183–190.

Bal-Price, A. K., Suñol, C., Weiss, D. G., van Vliet, E., Westerink, R. H. S., and Costa, L. G. (2008). Application of in vitro neurotoxicity testing for regulatory purposes: Symposium III summary and research needs. *Neurotoxicology* **29,** 520–531.

Berridge, M. J., Bootman, M. D., and Roderick, H. L. (2003). Calcium signalling: Dynamics, homeostasis and remodelling. *Nat. Rev. Mol. Cell Biol.* **4,** 517–529.

Boix, J., Cauli, O., and Felipo, V. (2010). Developmental exposure to polychlorinated biphenyls 52, 138 or 180 affects differentially learning or motor coordination in adult rats. Mechanisms involved. *Neuroscience* **167,** 994–1003.

Broding, H. C., Schettgen, T., Goen, T., Angerer, J., and Drexler, H. (2007). Development and verification of a toxicokinetic model of polychlorinated biphenyl elimination in persons working in a contaminated building. *Chemosphere* **68,** 1427–1434.

Carrasco, M. A., and Hidalgo, C. (2006). Calcium microdomains and gene expression in neurons and skeletal muscle cells. *Cell Calcium* **40,** 575–583.

Catterall, W. A., and Few, A. P. (2008). Calcium channel regulation and presynaptic plasticity. *Neuron* **59,** 882–901.

Danielsson, C., Harju, M., Halldin, K., Tysklind, M., and Andersson, P. L. (2008). Comparison of levels of PCDD/Fs and non-ortho PCBs in PCB153 from seven different suppliers. *Organ. Comp.* **70,** 201–203.

Deitmer, J. W., and Schild, D. (2000). Calcium-Imaging, Protocolle und Ergebnisse. In Ca2+ und pH, Ionenmessungen in Zellen und Geweben (J. W. Deitmer and D. Schild, Eds.), pp. 77–99. Spektrum Akademischer Verleger, Heidelberg, Germany.

Dingemans, M. M. L., Heusinkveld, H. J., de Groot, A., Bergman, A., van den Berg, M., and Westerink, R. H. S. (2009). Hexabromocyclododecane inhibits depolarisation-induced increase in intracellular calcium levels and neurotransmitter release in PC12 cells. *Toxicol. Sci.* **107,** 490–497.

European Food Safety Authority. (2005). Opinion of the scientific panel on contaminants in the food chain on a request from the commission related to the presence of non dioxin-like polychlorinated biphenyls (PCB) in feed and food. *EFSA J.* **284,** 1–137.

Eriksson, P., and Fredriksson, A. (1996). Developmental neurotoxicity of four ortho-substituted polychlorinated biphenyls in the neonatal mouse. *Environ. Toxicol. Pharmacol.* **1,** 155–165.

Faroon, O., Jones, D., and de Rosa, C. (2001). Effects of polychlorinated biphenyls on the nervous system. *Toxicol. Ind. Health* **16,** 305–333.

Fonnum, F., and Mariussen, E. (2009). Mechanisms involved in the neurotoxic effects of environmental toxicants such as polychlorinated biphenyls and brominated flame retardants. *J. Neurochem.* **111,** 1327–1347.

Gabrio, T., Piechotowski, I., Wallenhorst, T., Klett, M., Cott, L., Friebel, P., Link, B., and Schwenk, M. (2000). PCB-blood levels in teachers, working in PCB-contaminated schools. *Chemosphere* **40,** 1055–1062.

Garcia, A. G., Garcia-De-Diego, A. M., Gandia, L., Borges, R., and Garcia-Sancho, J. (2006). Calcium signaling and exocytosis in adrenal chromaffin cells. *Physiol. Rev.* **86,** 1093–1131.

Greene, L., and Tischler, A. (1976). Establishment of a noradrenergic clonal line of rat adrenal pheochromocytoma cells which respond to nerve growth factor. *Proc. Natl. Acad. Sci. U.S.A.* **73,** 2424–2428.

Harrad, S., Goosey, E., Desborough, J., Abdallah, M. A., Roosens, L., and Covaci, A. (2010). Dust from U.K. primary school classrooms and daycare centers: The significance of dust as a pathway of exposure of young U.K. children to brominated flame retardants and polychlorinated biphenyls. *Environ. Sci. Technol.* **44,** 4198–4202.

Hendriks, H. S., Antunes Fernandes, E. C., Bergman, A., van den Berg, M., and Westerink, R. H. S. (2010). PCB-47, PBDE-47, and 6-OH-PBDE-47 differentially modulate human $GABA_A$ and alpha4beta2 nicotinic acetylcholine receptors. *Toxicol. Sci.* **118,** 635–642.

Holene, E., Nafstad, I., Skaare, J. U., and Sagvolden, T. (1998). Behavioural hyperactivity in rats following postnatal exposure to sub-toxic doses of polychlorinated biphenyl congeners 153 and 126. *Behav. Brain Res.* **94,** 213–224.

Hondebrink, L., Meulenbelt, J., Meijer, M., van den Berg, M., and Westerink, R. H. S. (2011). High concentrations of MDMA ('ecstasy') and its metabolite MDA inhibit calcium influx and depolarisation-evoked vesicular dopamine release in PC12 cells. *Neuropharmacology* **61,** 202–208.

Inglefield, J. R., Mundy, W. R., and Shafer, T. J. (2001). Inositol 1,4,5-triphosphate receptor-sensitive Ca(2+) release, store-operated Ca(2+) entry, and cAMP responsive element binding protein phosphorylation in developing cortical cells following exposure to polychlorinated biphenyls. *J. Pharmacol. Exp. Ther.* **297,** 762–773.

Khadikar, P. V., Singh, S., and Shrivastava, A. (2002). Novel estimation of lipophilic behaviour of polychlorinated biphenyls. *Bioorg. Med. Chem. Lett.* **12,** 1125–1128.

Malenka, R. C., and Nicoll, R. A. (1999). Long-term potentiation—A decade of progress? *Science* **285,** 1870–1874.

Mattson, M. P. (2007). Calcium and neurodegeneration. *Aging Cell* **6,** 337–350.

Michaelsen, K., and Lohmann, C. (2010). Calcium dynamics at developing synapses: Mechanisms and functions. *Eur. J. Neurosci.* **32,** 218–223.

Orrenius, S., Nicotera, P., and Zhivotovsky, B. (2011). Cell death mechanisms and their implications in toxicology. *Toxicol. Sci.* **119,** 3–19.

Pessah, I. N., Cherednichenko, G., and Lein, P. J. (2010). Minding the calcium store: Ryanodine receptor activation as a convergent mechanism of PCB toxicity. *Pharmacol. Ther.* **125,** 260–285.

Pessah, I. N., Hansen, L. G., Albertson, T. E., Garner, C. E., Ta, T. A., Do, Z., Kim, K. H., and Wong, P. W. (2006). Structure-activity relationship for noncoplanar polychlorinated biphenyl congeners toward the ryanodine receptor-Ca2+ channel complex type 1 (RyR1). *Chem. Res. Toxicol.* **19,** 92–101.

Petrik, J., Drobna, B., Pavuk, M., Jursa, S., Wimmerova, S., and Chovancova, J. (2006). Serum PCBs and organochlorine pesticides in Slovakia: Age, gender, and residence as determinants of organochlorine concentrations. *Chemosphere* **65,** 410–418.

Safe, S. (1993). Toxicology, structure-function relationship, and human and environmental health impacts of polychlorinated biphenyls: Progress and problems. *Environ. Health Perspect.* **100,** 259–268.

Schantz, S. L., Widholm, J. J., and Rice, D. C. (2003). Effects of PCB exposure on neuropsychological function in children. *Environ. Health Perspect.* **111,** 357–376.

Stenberg, M., and Andersson, P. L. (2008). Selection of non-dioxin-like PCBs for in vitro testing on the basis of environmental abundance and molecular structure. *Chemosphere* **71,** 1909–1915.

Tilson, H. A., and Kodavanti, P. R. (1998). The neurotoxicity of polychlorinated biphenyls. *Neurotoxicology* **19,** 517–525.

Van den Berg, M., Birnbaum, L. S., Denison, M., De Vito, M., Farland, W., Feeley, M., Fiedler, H., Hakansson, H., Hanberg, A., Haws, L., *et al.* (2006). The 2005 World Health Organization reevaluation of human and mammalian toxic equivalency factors for dioxins and dioxin-like compounds. *Toxicol. Sci.* **93,** 223–241.

Westerink, R. H. S. (2006). Targeting exocytosis: Ins and outs of the modulation of quantal dopamine release. *CNS Neurol. Disord. Drug Targets* **5,** 57–77.

Westerink, R. H. S., and Ewing, A. G. (2008). The PC12 cell as model for neurosecretion. *Acta Physiol.* **192,** 273–285.

Winneke, G., Walkowiak, J., and Lilienthal, H. (2002). PCB-induced neurodevelopmental toxicity in human infants and its potential mediation by endocrine dysfunction. *Toxicology* **181–182,** 161–165.

Wong, P. W., Garcia, E. F., and Pessah, I. N. (2001). Ortho-substituted PCB95 alters intracellular calcium signaling and causes cellular acidification in PC12 cells by an immunophilin-dependent mechanism. *J. Neurochem.* **76,** 450–463.

Wong, P. W., and Pessah, I. N. (1997). Noncoplanar PCB 95 alters microsomal calcium transport by an immunophilin FKBP12-dependent mechanism. *Mol. Pharmacol.* **51,** 693–702.